AIP Applied Physics Letters

Effect of microstructural change on magnetic property of Mn-implanted p-type GaN

Jeong Min Baik, Ho Won Jang, Jong Kyu Kim, and Jong-Lam Lee

Citation: Applied Physics Letters **82**, 583 (2003); doi: 10.1063/1.1541111

View online: http://dx.doi.org/10.1063/1.1541111

View Table of Contents: http://scitation.aip.org/content/aip/journal/apl/82/4?ver=pdfcov

Published by the AIP Publishing

Effect of microstructural change on magnetic property of Mn-implanted *p*-type GaN

Jeong Min Baik, Ho Won Jang, Jong Kyu Kim, and Jong-Lam Lee[a)]
Department of Materials Science and Engineering, Pohang University of Science and Technology (POSTECH), Pohang, Kyungbuk 790-784, Korea

(Received 26 August 2002; accepted 9 December 2002)

A dilute magnetic semiconductor was achieved by implanting Mn ions into *p*-type GaN and subsequent annealing. The ferromagnetic property was obtained after annealing at 800 °C. This was attributed to the formation of Ga–Mn magnetic phases. Higher temperature annealing at 900 °C reduced the ferromagnetic signal and produced antiferromagnetic Mn–N compounds such as $Mn_6N_{2.58}$ and Mn_3N_2, leaving N vacancies. This provides evidence that N vacancies play a critical role in weakening the ferromagnetic property in the Mn-implanted GaN. © *2003 American Institute of Physics.* [DOI: 10.1063/1.1541111]

Recently, dilute magnetic semiconductors (DMSs) based on III–V semiconductors have attracted a great deal of attention because of their application to magnetic semiconductor devices such as spin-field-effect transistors and spin-light-emitting diodes.[1–3] In particular, (Ga,Mn)N is a very promising material because its Curie temperature is higher than room temperature according to the theoretical calculation.[4] This allows the spintronic devices to operate at room temperature. Highly Mn-doped GaN film ($\geqslant 10^{21}/cm^3$) showing ferromagnetic behavior was successfully grown on sapphire (0001) by molecular-beam epitaxy (MBE).[5] The ferromagnetic property was also reported in Mn-implanted GaN with subsquent annealing.[6,7] Based on the material characterization using x-ray diffraction (XRD) and/or transmission electron microscopy, it was proposed that (Ga,Mn)N solid solution and/or Ga–Mn binary phases could play a major role in emerging the ferromagnetic property in the Mn-doped GaN films. However, no clear evidence on the existence of such secondary phases has been experimentally provided because of the lack of experimental resolution. Meanwhile, x-ray scattering and photoemission spectroscopy using synchrotron radiation could provide quantitative information about the chemical and electronic properties, which should be crucial for the understanding of the origin of ferromagnetic properties in GaN-based DMS.

In this work, we studied microstructural evolution of Mn-implanted *p*-type GaN as a function of annealing temperature. Synchrotron XRD and synchrotron radiation photoemission spectroscopy (SRPES) were employed to identify secondary phases and chemical bonding states in the Mn-implanted and annealed *p*-type GaN. From these results, the effect of microstructural change on the magnetic property of Mn-implanted *p*-type GaN is discussed.

The GaN films used in this work were grown by metal-organic chemical deposition on a (0001) sapphire substrate. An undoped GaN layer with a thickness of 1 μm was grown, followed by a growth of 1-μm-thick *p*-type GaN doped with Mg. Electrical activation of the grown samples was carried out at 750 °C for 4 min by rapid thermal annealing under an N_2 atmosphere. The net hole concentration in the film was determined to be 2.5×10^{17} cm^{-3} by Hall measurements. After the growth of the films, Mn^+ ions were implanted into the *p*-type GaN films with an energy of 180 keV and dose of 5×10^{16} cm^{-2}. All samples were held at 350 °C during the implantation to avoid amorphization. Subsequent annealing at 800 and 900 °C for 30 s was performed under flowing N_2 gas in a face-to-face condition. The magnetization measurement was carried out using a superconducting quantum interference device magnetometer (MPMSXL, Quantum Design Co., Ltd).

Figure 1 shows magnetization curves at 10 K for samples annealed at 800 and 900 °C. The magnetization curves were obtained with the applied field parallel to the plane of the samples. The diamagnetic background of GaN substrate was subtracted. The hysteresis loops showed clear ferromagnetic behavior of the samples. It is clearly shown in Fig. 1 that the ferromagnetic signal for the 800 °C-annealed sample was stronger than that for the 900 °C-annealed one. The coercive field increased from 40 to 79 Oe, while the residual magnetization decreased from 1.75×10^{-3} to 7.75×10^{-4} emu/g with annealing temperature.

Figure 2 shows XRD profiles of Mn-implanted GaN

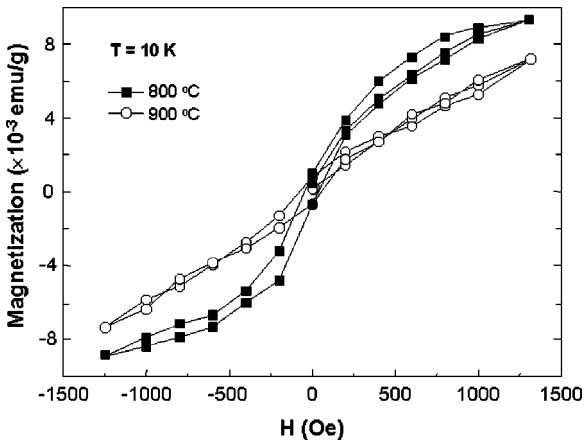

FIG. 1. Magnetization curves for Mn-implanted samples with annealing temperature.

a)Electronic mail: jllee@postech.ac.kr

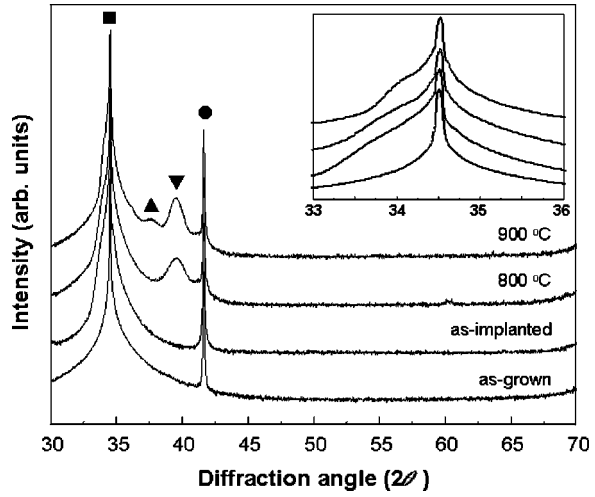

FIG. 2. Change of XRD scans of Mn-implantated GaN with annealing temperature. The inset shows the expanded view at around GaN (0002) peak; (■) GaN, (●) Al_2O_3, (▼) $Mn_6N_{2.58}$, and (▲) Mn_3N_2.

samples with annealing temperature. Compared to the as-grown sample, no reaction between Mn and GaN was observed in the as-implanted one. After annealing at 800 °C, a Mn–N compound of $Mn_6N_{2.58}$ was produced. When the sample was annealed at 900 °C, the $Mn_6N_{2.58}$ peak intensity increased and a new peak corresponding to Mn_3N_2 was observed. The inset in Fig. 2 shows enlarged XRD scans ranging from $2\theta = 33°$ to 36°. A shoulder was found at the lower angle side of the GaN (0002) peak and its intensity became large at a higher annealing temperature. The shoulder could attribute to the strain along the GaN *c* axis, resulting from the decrease in implantation-induced damage during annealing.[8]

Figure 3 shows the change of the SRPES spectra of Mn $2p_{3/2}$ and Ga $3d$ core levels with annealing temperature. In order to remove surface oxides, the samples were *in situ* etched about 50 Å using Ar ion sputtering. Only one peak was observed in the Mn $2p_{3/2}$ spectra for both as-implanted and 900 °C-annealed samples, as shown in Fig. 3(a). The peak corresponds to Mn—N bond considering the XRD data in Fig. 2. In the sample annealed at 800 °C, a new peak locates at the lower binding energy by about 3.0 eV. This could be either metallic Mn—Mn (Ref. 9) or Ga—Mn bonds. The origin of the peak was revealed by the SRPES spectra of Ga $3d$, shown in Fig. 3(b). The Ga $3d$ spectrum of

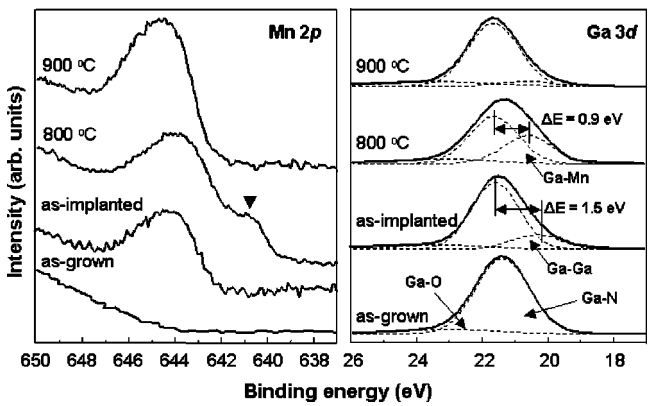

FIG. 3. Change of the SRPES spectra for (a) Mn $2p_{3/2}$ and (b) Ga $3d$ core levels in Mn-implanted and annealed GaN.

TABLE I. Relative concentrations (%) of chemical bonds determined from the Ga $3d$ SRPES spectra in Fig. 3(b). The bracketed values represent the FWHM value of each bond.

Sample	Ga—N (1.52 eV)	Ga—O (2.71 eV)	Ga—Ga (1.42 eV)	Ga—Mn (1.50 eV)
As-grown	91.2	8.8	···	···
As-implanted	81.9	10.1	8.0	···
800 °C	63.4	10.3	···	26.3
900 °C	80.9	13.0	···	6.1

the as-grown sample consists of Ga—N and Ga—O bonds. After the Mn implantation, the spectrum shows asymmetry at the lower bonding energy of the Ga—N bond. The full width at half maximum (FWHM) value of Ga $3d$ peak was measured to be 1.65 eV for the as-grown *p*-type GaN, but 1.95 eV for the 800 °C-annealed *p*-type GaN. This means that an additional bonding is superimposed in the Ga $3d$ spectra. For the Mn-implanted sample, the superimposed peak could be attributed to metallic Ga atoms in GaN due to the implantation-induced loss of nitrogen atoms.[10] The difference of binding energy between Ga—N and Ga—Ga bonds is in good agreement with the reported value of 1.7 eV.[11] For the sample annealed at 800 °C, a new peak could be separated at the lower bonding energy by 0.9 eV relative to the peak of Ga—N bonds. The Ga atoms in the Mn-implanted sample could make bonding with N, O, and Mn atoms, such as Ga—N, Ga—O, and Ga—Mn bonds, respectively. Considering the electron negativity of each element, the Ga—Mn bond should be located between the Ga—N and Ga—Ga bonds.[11] Therefore, the new peak in the 800 °C-annealed sample should originate from the Ga—Mn bond. After annealing at 900 °C, the peak intensity for the Ga—Mn bond decreased drastically. FWHM values and relative concentrations of deconvoluted peaks in the Ga $3d$ spectra are summarized in Table I. Meanwhile, the relative atomic ratio of Ga/N was determined from integrating intensities in the Ga $3d$ and N $1s$ spectra, summarized in Table II. The ratio measured at a detection angle $\theta = 90°$ in an as-implanted sample was set as 1.0 for reference. As the annealing temperature increases, the Ga/N increases, meaning the production of N vacancies in the annealed GaN. At a smaller θ, the intensity of photoelectrons emitting from the surface becomes dominant due to the inelastic mean-free path of photoelectrons. At $\theta = 30°$, the increase in Ga/N ratio with annealing temperature was more pronounced. This supports that nitrogen atoms were preferentially diffused out to the surface during annealing, leaving N vacancies near the surface region.

The change of surface band bending with annealing temperature was observed from valence band spectra, as shown in Fig. 4. The Fermi level was determined by linearly extrapolating the sloped region with the base line in the valence

TABLE II. Change of Ga/N atomic ratio with the detection angle, θ.

θ	As-implanted	800 °C	900 °C
90°	1	1.08	1.16
60°	1.08	1.41	1.53
30°	1.34	1.91	2.25

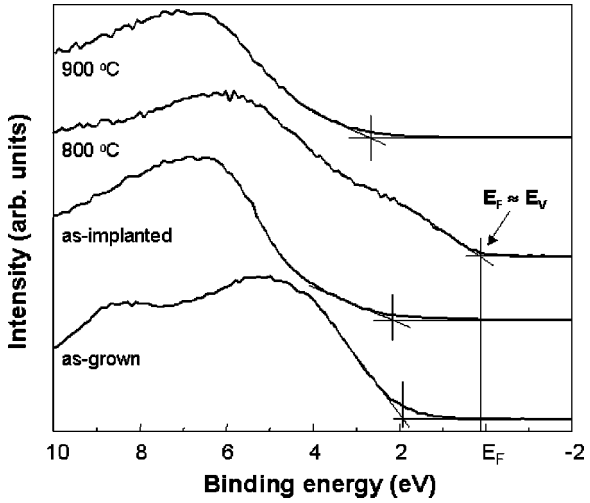

FIG. 4. Change of valence band spectra of Mn-implanted GaN with annealing temperature.

band spectrum of Au foil, defined as the level of zero-binding energy. For the sample annealed at 900 °C, the Fermi level shifts by 0.5 eV toward conduction band in comparison with the as-implanted sample. This is related to N vacancies produced during annealing[10] because N vacancies act as donors for electrons.[12] However, after annealing at 800 °C, the Fermi level nearly coincides with the valence band maximum. This is due to the fact that the surface of the Mn-implanted sample changed into metallic surface, consistent with the observation of metallic Ga—Mn bonds in Figs. 3(a) and 3(b).

The change of magnetic properties with annealing temperature could be explained in terms of the microstructural point of view, deduced from Figs. 3 and 4. At the higher annealing temperature at 900 °C, Mn–N compounds, such as Mn_3N_2 and $Mn_6N_{2.58}$, were produced, leaving N vacancies behind. This was evidenced that the Ga/N ratio at $\theta = 90°$ increased with annealing temperature (Table II). These Mn–N compounds are known as antiferromagnetic materials with Neél temperature above 300 K,[13,14] reducing the magnetic moment of the Mn-implanted GaN. In addition, N vacancies have shallow donor levels, located at about 30–40 meV below the conduction band edge.[12] Thus, some part of the holes compensated with electrons generated from N vacancies led to the reduction of hole concentration. It was reported that the holes mediate the long-range interactions between the localized spins in the III–V magnetic semiconductors, enhancing the ferromagnetic properties of the materials.[1] Therefore, the ferromagnetic signal reduced as the concentration of N vacancies increased.

It was shown that the ferromagnetic behavior found after annealing at 800 °C originated from the Ga—Mn bond [Fig. 3(a)] even though such phases were not identified from XRD measurements [Fig. 2]. It was reported that the ferromagnetic behavior of Mn-implanted GaN could be due to the formation of Mn_3Ga phase.[7] Thus, it is proposed that the Ga—Mn bond could originate from a binary phase of Ga—Mn. No observation of such a Ga—Mn phase might be attributed to the nanoscale size[7] and the Ga—Mn magnetic phases with random orientation. The Ga—Mn magnetic phases disappeared as the annealing temperature increased to 900 °C. This could be explained to result from the decrease in Mn concentration in GaN associated with the precipitation of Mn nitride. From this, it is suggested that optimum annealing temperature (<900 °C) could be an important parameter in enhancing the ferromagnetism in the Mn-implanted and annealed GaN by suppressing the production of N vacancies.

In conclusion, the Ga—Mn magnetic phases contributing to the ferromagnetic property were produced after annealing Mn-implanted *p*-type GaN at 800 °C. The increase in the annealing temperature to 900 °C promoted the formation of antiferromagnetic Mn–N compounds such as $Mn_6N_{2.58}$ and Mn_3N_2, leaving N vacancies near the surface region. The results suggest that the ferromagnetic property could be enhanced by an optimizing annealing temperature (<900 °C) to avoid the predominant reaction of Mn atoms with N.

The authors would like to thank M. S. Park for useful advice and technical support. This work was supported in part by Korea Science and Engineering Foundation through the Quantum-functional Semiconductor Research Center at Dongguk University in 2002, and in part by the project for ''National Research Laboratory'' sponsored by the Korea Institute of Science and Technology Evaluation and Planning (KISTEP). High-resolution XRD and SRPES using synchrotron radiation were carried out at the 3C2 and 8A1 SPEM beamlines at Pohang Accelerator Laboratory (PAL), respectively.

[1] H. Ohno, Science **281**, 951 (1998).
[2] H. Ohno, A. Shen, F. Matsukura, A. Oiwa, A. Endo, S. Katsumoto, and Y. Iye, Appl. Phys. Lett. **69**, 363 (1996).
[3] M. L. Reed, N. A. El-Masry, H. H. Stadelmaier, M. K. Ritums, M. J. Reed, C. A. Parker, J. C. Roberts, and S. M. Bedair, Appl. Phys. Lett. **79**, 3473 (2001).
[4] T. Diel, H. Ohno, F. Matsukura, J. Cibert, and D. Ferrand, Science **287**, 1019 (2000).
[5] S. Sonoda, S. Shimizu, T. Sasaki, Y. Yamamoto, and H. Hori, J. Cryst. Growth **237**, 1358 (2002).
[6] Y. Shon, Y. H. Kwon, D. Y. Kim, X. Fan, D. Fu, and T. W. Kang, Jpn. J. Appl. Phys., Part 1 **40**, 5304 (2001).
[7] N. Theodoropoulou, A. F. Hebard, M. E. Overberg, C. R. Abernathy, S. J. Pearton, S. N. G. Chu, and R. G. Wilson, Appl. Phys. Lett. **78**, 3475 (2001).
[8] B. J. Pong, C. J. Pan, Y. C. Teng, G. C. Chi, W.-H. Li, K. C. Lee, and C.-H. Lee, J. Appl. Phys. **83**, 5992 (1998).
[9] I. Wu and A. Kahn, J. Vac. Sci. Technol. B **16**, 2218 (1998).
[10] Y. Nakano and T. Kachi, Appl. Phys. Lett. **79**, 1468 (2001).
[11] J. F. Mouler, W. F. Strickle, P. E. Sobol, and K. D. Bomben, *Handbook of X-Ray Photoelectron Spectroscopy* (Perkin–Elmer, Eden Prairie, MN, 1992).
[12] P. Boguslawski, E. L. Briggs, and J. Bernholc, Phys. Rev. B **51**, 17255 (1995).
[13] H. Yang, H. Al-Brithen, E. Trifan, D. C. Ingram, and A. R. Smith, J. Appl. Phys. **91**, 1053 (2002).
[14] M. N. Eddine and E. F. Bertaut, Solid State Commun. **23**, 147 (1977).